JAERI-Research
2003-019

JP0350570

FEASIBILITY STUDY OF THE WATER CHERENKOV DETECTOR AS A D-T FUSION POWER MONITOR IN THE SYSTEM USING NEUTRON ACTIVATION OF FLOWING WATER - FIRST EXPERIMENTAL PHASE -

September 2003

Yury M. VERZILOV*, Kentaro OCHIAI and Takeo NISHITANI

日本原子力研究所
Japan Atomic Energy Research Institute

本レポートは，日本原子力研究所が不定期に公刊している研究報告書です。
入手の問合わせは，日本原子力研究所研究情報部研究情報課（〒319-1195 茨城県那珂郡東海村）あて，お申し越しください。なお，このほかに財団法人原子力弘済会資料センター（〒319-1195 茨城県那珂郡東海村日本原子力研究所内）で複写による実費頒布をおこなっております。

This report is issued irregularly.
Inquiries about availability of the reports should be addressed to Research Information Division, Department of Intellectual Resources, Japan Atomic Energy Research Institute, Tokai-mura, Naka-gun, Ibarakiken 319-1195, Japan.

© Japan Atomic Energy Research Institute, 2003
編集兼発行　日本原子力研究所

Feasibility Study of the Water Cherenkov Detector as a D-T Fusion Power Monitor in the System using Neutron Activation of Flowing Water
− First Experimental Phase −

Yury M.VERZILOV*, Kentaro OCHIAI and Takeo NISHITANI

Department of Fusion Engineering Research
(Tokai Site)
Naka Fusion Research Establishment
Japan Atomic Energy Research Institute
Tokai-mura, Naka-gun, Ibaraki-ken

(Received August 1, 2003)

The technique of monitoring D-T neutrons using water flow is based on the reaction of the $^{16}O(n,p)^{16}N$. In order to significantly improve the D-T neutron monitoring system in the ITER reactor in comparison with the system that uses a γ-ray scintillation detector, a new approach was proposed. The basic idea of this approach is to utilize the Cherenkov light, produced by energetic β-particles from ^{16}N in water near the first wall of the fusion reactor, and then deliver the light by the optical fiber to the remote light detector. The proof of the principle experiment is divided into two phases. The main idea of the first experimental phase is to examine Cherenkov light measurements using a remotely located water radiator and light detector. During the second phase the water radiator will be placed next to the neutron source, then the Cherenkov light will be transferred by an optical fiber to the remotely located light detector. For the purpose of the first experimental phase, a water Cherenkov detector was installed in the shielded measurement room. A closed water loop, with circulating water, was used to transport ^{16}N from the D-T neutron source to the Cherenkov detector. The experiment was carried out at FNS/JAERI, with the accelerator set to a direct current mode, the source neutron yield around 2×10^{11} n/s, and the water flowage approximately 2 m/s. The registered Cherenkov signal was identified as the light produced by β-particles from ^{16}N using the time decay and the energy spectra data. According to the present study, the water Cherenkov detector is very effective for measurements of the ^{16}N activity, due to high counting efficiency, absence of the scintillation detector and simplicity of the method.

Keywords: D-T Neutrons, Fusion Reactor, Neutron Monitor, ITER, FNS, Water Activation, Nitrogen-16, Cherenkov Light

---

* JAERI Research Fellow

流水の放射化を利用した核融合出力モニター用検出器としての水チェレンコフ検出器の成立性に関する研究 —第１次実験—

日本原子力研究所那珂研究所核融合工学部
Yury M.VERZILOV*・落合　謙太郎・西谷　健夫

(2003年８月１日受理)

流水を用いた中性子モニター法は $^{16}O(n,p)^{16}N$ 反応に基づいている。本研究ではシンチレーションγ線検出器を用いた ITER の中性子モニターシステムを著しく改善するための新しい手法を提案する。基本的概念は核融合炉の真空容器近傍の水中で生成される ^{16}N からのβ粒子によるチェレンコフ光を光ファイバーで外部に引き出し、光検出器で計測するものである。その原理実証実験を２段階に分けて実施する。まず第１次実験では、よく遮蔽された測定室において照射された水からのチェレンコフ光の測定できることを確認する。第２段階では、水を中性子源近傍に設置し、照射下のチェレンコフ光を光ファイバーで伝送して測定する。第１次実験は原研 FNS で実施し、チェレンコフ光検出器を良く遮蔽された測定室に設置した。FNS 加速器は直流モードで運転し、中性子発生率は約 2×10^{11} n/s、水ループの流速は約 1 m/s であった。測定された信号はエネルギースペクトルと減衰時間から、^{16}N のβ粒子によるチェレンコフ光によるものであると確認した。本研究により、水チェレンコフ検出器は計数効率が高く、さらにシンチレーション検出器を必要としない簡便な手法であるため、^{16}N の検出器として有用であることを示した。

那珂研究所（東海駐在）：〒319-1195 茨城県那珂郡東海村白方白根 2-4
*　　原研リサーチフェロー

Contents

目　次

1. Introduction

The neutron activation of the ^{16}O via $^{16}O(n,p)^{16}N$ reaction and subsequent γ-ray detection of the ^{16}N activity in a flowing fluid was applied for a variety of purposes, for example: on-line oxygen analysis, flow rate measurements[1]. Since the threshold energy for the $^{16}O(n,p)^{16}N$ reaction is 10.24 MeV[2], ^{16}N nuclei is practically produced only by the 14 MeV neutrons, when water flows in the vicinity of the D-T neutron source. Therefore, a fusion power monitor based on activation of flowing water was proposed for ITER and experimental studies were completed[3-5].

The activation product, ^{16}N, decays by beta emission (100%) with a half-life of 7.13 seconds, Table 1[6].

Table 1. Radioactive decay properties* of ^{16}N ($T_{1/2}$ = 7.13 sec)

Ray	E_β endpoint (keV) E_γ (keV)	I_β (%) I_γ (%)	Decay mode
Beta	1548.1	1.06	β^-
	3303.2	4.8	
	4290.1	66.2	
	10420	28.0	
Gamma	6128.63	67	
	7115.15	4.9	

* Only branches with intensities of more than 1 % are listed in the table.

The main branch produces a β-particle with an endpoint energy of 4.290 MeV (66.2%) and a 6.128 MeV γ-ray. Another branch produces a 7.115 MeV γ-ray in coincidence with β-particles, whose endpoint energy is 3.303 MeV (4.8%). The direct branch to the ground state produces a β-particle with endpoint energy of 10.42 MeV (28%) without an associated γ-ray.

Presently, activity of the ^{16}N is measured using a γ-ray scintillation detector[3-5]. Such method leads to insufficient time resolution and the delaying of the neutron monitor response, since water has to transfer the ^{16}N from the point of production to the position of a remote γ-detector. To overcome these disadvantages a new approach was proposed. The basic idea of this approach is to utilize the Cherenkov light, produced by energetic β-particles from ^{16}N in water near the first wall of the fusion reactor, and then transmit the light by the optical fiber to the remote light detector.

The proof of the principle experiment is divided into two phases. The main idea of the first experimental phase is to examine the Cherenkov light measurements using a remotely located water radiator and a light detector. During the second phase the water radiator is placed next to the neutron source, and then the Cherenkov light will be transmitted by an optical fiber to the remotely located light detector. In the present report, theoretical considerations and experimental investigations of the first experimental phase are presented.

2. Theoretical aspects of a water Cherenkov detector

Water has been chosen for the Cherenkov radiator for a number of reasons. First of all, water cools the fusion reactor and the water Cherenkov detector can be easily implemented to the reactor system. The refraction index of water provides a Cherenkov threshold for low-energy particles. In addition, water has a long light attenuation length, does not scintillate, is chemically inert, nonvolatile, and is able to perform superior radiation shielding.

2.1. Light emission

Cherenkov emission is a physical process.[7,8] Several important properties of the Cherenkov light should be taken into account for further consideration. Electrons emit light under a characteristic angle when passing through the medium of the refraction index n, if their velocity exceeds the speed of light, c/n. Translating this condition into a relativistic energy expression yields the threshold energy E_{th} for electrons:

$$E_{th} = 0.511\left(\frac{1}{\sqrt{1-1/n^2}} - 1\right). \quad (1)$$

For water (n=1.33) the threshold energy is 0.264 MeV. The Cherenkov angle of θ is related to the electron velocity v and the refractive index of the medium n:

$$\cos\theta = \frac{1}{n \cdot \beta}, \quad (2)$$

where $\beta = v/c$.

The Cherenkov light in water is emitted under 42° by β-rays coming from the ^{16}N, Figure 1.

According to the classical description of the Cherenkov effect by Frank and Tamm[9] the number of photons dN emitted per unit path length dx with wavelengths between λ_1 and λ_2 is given by:

$$\frac{dN}{dx} = 2\pi\alpha z^2 \int_{\lambda_1}^{\lambda_2}\left(1 - \frac{1}{n^2\beta^2}\right)\frac{d\lambda}{\lambda^2}, \quad (3)$$

for $n(\lambda) > 1$, where z is the electric charge of the particle producing Cherenkov radiation and $\alpha = 1/137$ is a fine structure constant. Although the number of emitted Cherenkov photons exhibits a $1/\lambda^2$ dependence, equation (3), Cherenkov photons are not emitted in the X-ray range due to the refraction index of n=1 in this region, therefore the condition necessary for Cherenkov emission cannot be fulfilled.

Assuming that a photomultiplier tube with a bialkali photocathode will be utilized for registration of the Cherenkov light, the spectral range of the maximum response can be estimated as follows. Figure 2 (curve A) shows the calculated

Cherenkov spectrum expressed in terms of the number of generated photons, which is proportional to $1/\lambda^2$. Curve B shows the spectral response for a photomultiplier tube (Hamamatsu R1250) containing a bialkali photocathode. The product of curves A and B (curve C) shows the number of photoelectrons, liberated at the photo-cathode, when Cherenkov light irradiates the cathode. Considering the curve C, it is possible to conclude that the region of the maximum response is estimated to be in the range of 300 – 600 nm. The area under the curve C represents the total number of photoelectrons liberated. This will depend upon the initial energy of the particle, permitting pulse height analysis of the pulse distribution, recorded from a mixture containing β-emitting radionuclides of different energies.

2.2. Estimating light intensity

To obtain the quanta of Cherenkov photons produced in water by the electron with energy of E_{max} (MeV), equation (3) must be integrated over the spectral region and the energy range from the Cherenkov threshold to the E_{max}. The spectral region (300 – 600 nm) was determined from the maximum response of the photomultiplier tube point of view. For simplicity, it was assumed that the refraction index of water for this range is constant, being equal to 1.33. The spectral integration of equation (3) gives the number of Cherenkov photons emitted by an electron with energy E per unit path, with wavelengths between 300 – 600 nm. This formula summarizes the equation:

$$\frac{dN}{dx} = 764.4 \cdot \left(1 - \frac{1}{(vn/c)^2}\right). \tag{4}$$

In the case of electrons in water, x is a function of the original electron energy. This equation has to be converted to a dN/dE form with the use of the $v(E)$ and $x(E)$ expressions, for integration over the mentioned energy range. The v(E) expression can be derived as:

$$v(E) = c\sqrt{1 - \left(\frac{1}{(E/0.511)+1}\right)^2}. \tag{5}$$

An empirical relation of the range and energy of electrons in water was established from experimental data[10]. In the interval ~ 0.3 to 12 MeV the range x (cm) is given by

$$x(E) \approx (0.530E - 0.106). \tag{6}$$

The calculated range for electrons from ^{16}N in water is presented in Figure 3. In case of water, this formula gives the maximum margin of error ±15 percent for the low electron energies, however their contribution in the Cherenkov light production is insignificant, thus the empirical relation gives an accurate estimation. Taking into account the expressions (5) and (6), the final equation is:

(7)

$$\frac{dN}{dE} = 405.1 \cdot \left(1 - \frac{1}{\left[1 - 1/\left(\frac{E}{0.511} + 1 \right)^2 \right] n^2} \right),$$

The equation (7) was integrated numerically. The obtained data is shown in Figure 4. The data represents the number of Cherenkov photons that will be produced by the electron, moderating in water from E_{max} to the Cherenkov threshold (0.264 MeV). For future estimations, the calculated data was approximated by polynomial function on the energy range of Cherenkov threshold in water and the maximum energy of electrons from β-decay of ^{16}N. The following formula was established:

(8)

$$N(E) = 8.68\times10^{-14} \cdot E^4 - 2.14\times10^{-9} \cdot E^3 + 1.85\times10^{-5} \cdot E^2 + 1.09\times10^{-1} \cdot E - 3.37\times10^{1}$$

The emitted Cherenkov spectrum data for various electron energies was also calculated. An example of the Cherenkov spectra for an electron with a maximum energy of 4.0 Mev is shown in Figure 5. The obtained result agrees with the data from an earlier study[11].

2.3. Cherenkov yield

The Cherenkov yield η (%) for beta radionuclides is determined by the ratio of the number of electrons in the energy range of Cherenkov threshold to the endpoint energy, and the total number of electrons in the beta spectrum:

(9)

$$\eta = \frac{\int_{E_{th}^{Ch}}^{E_{max}} N(E)dE}{\int_{0}^{E_{max}} N(E)dE} \cdot 100$$

In addition to the endpoint energy, some other variables are implicated in the determination of the Cherenkov counting efficiency. According to the Fermi theory of beta disintegration[12], the β-particle energy-distribution depends on the nuclear Coulomb field, spin variation, and the parity change. Thus, to obtain the correct value of Cherenkov yield, the shape of the beta spectrum has to be taken into account. The number of electrons *N(E)* can be calculated with the help of a polynomial approximation of the Fermi function describing the distribution of beta particles per energy interval unit. In this study two selected radionuclides, ^{16}N and ^{32}P, are considered. The β-ray spectrum of ^{32}P and ^{16}N is shown on Figure 6, with data obtained from the Reference[13]. The radionuclide ^{32}P was chosen for calibration of the water Cherenkov detector and estimation of the PMT response function. Integrations

of the Fermi function and the calculation of η by equation (9) gave the Cherenkov yield of 98.6 % for ^{16}N and 86.5 % for ^{32}P.

2.4. Simulation of the photomultiplier response

To obtain a realistic PMT response to Cherenkov photons from β-spectrum of ^{16}N in water, with an appropriate theory model, absolute calibration of the spectrometric channel must be done. This calibration is not presented in this study; therefore two assumptions are used to predict the qualitative pulse height spectrum of the PMT. First assumption concerns simplifying the β-spectrum, and the second one – the parameters and regime of the PMT.

The number of photoelectrons produced the PMT response was estimated in such a way. The real β-spectrum of ^{16}N is represented by four groups of β-rays, according to four branches with appropriate intensities, listed in Table 1. The average energy of electrons (E_{av}) in each group was evaluated using Fermi distribution. The number of Cherenkov photons *(M)* per electron with E_{av} was estimated by equation 8. The product of Cherenkov photons and the branch intensity, M x I_β, represents the amount of Cherenkov photons produced by electron with E_{av}. The results of the calculations are shown in Table 2.

Table 2. The number of photoelectrons produced by Cherenkov photons emitted per β-particle from decay of ^{16}N and ^{32}P.

Nuc-lide	Group number	E_β endpoint (keV)	Branch Intensity, I_β (%)	E_β average (keV)	Quanta of photons per β-particle, M	M x I_β	Quanta of photo-electrons, μ
^{16}N	1	1548.1	1.06	629.3	42	0.045	7.2E-3
	2	3303.2	4.80	1342.7	141	6.76	1.08
	3	4290.1	66.2	1743.8	202	133	21.3
	4	10420	28.0	4235.8	625	175	28
	Total	-	-	-	-	315	50
^{32}P	1	1710	100	695.1	50	50	8.0

Table 2 indicates that the ^{16}N decay generates two kinds of intensive events, one event producing 133 Cherenkov photons, and the second one – 175 photons. Beta-particle from the ^{32}P produces 50 Cherenkov photons. At last, the total number of photo electrons produced by β-particle from decay of ^{16}N and ^{32}P can be estimated by multiplying the total number of Cherenkov photons by the quantum efficiency of the PMT. The average quantum efficiency of photocathode of the PMT on the spectral range of 300 – 600 nm was estimated to be equal to 16%. Final results, including quantum efficiency of the photocathode, are shown in Table 2.

The qualitative response of the PMT is an estimation based on the quanta of photoelectrons (Table 2) and another assumption. In the second assumption, the simulation of the PMT response was based on data obtained for the EMI-9814B photomultiplier, working in the regime of single photoelectron analysis[14]. It is

concluded[14], that for high (more than 10^6) gains of the PMT, the response initiated by more than one photoelectron can be represented by the Gaussian approximation,

$$S(x) = \frac{1}{\sqrt{2\pi\mu\left(\sigma_1^2 + Q_1^2\right)}} \cdot \exp\left(-\frac{(x - Q_0 - Q_{sh} - \mu Q_1)^2}{2\mu\left(\sigma_1^2 + Q_1^2\right)}\right), \tag{10}$$

where: $\mu = m \cdot q$ - the number of photoelectrons emitted from the photocathode;
m – the mean number of photons hitting the photocathode;
q – the quantum efficiency of the photocathode.

The parameters of this distribution slightly depend on the light intensity. For estimation purposes average parameters (Q_0 = 23; σ_1 = 12; Q_1 = 23; Q_{sh} = 23) were used. Physical interpretation of these parameters: Q_0 – the pedestal; Q_{sh} – the effective spectrum shift due to background; Q_1 - the average charge at the PMT output when one electron is collected by the first dynode; σ_1 - the corresponding standard deviation of the charge distribution.

By comparing the number of photoelectrons (μ) produced by each group of β-rays with the other, it is possible to conclude that the main contribution to the PMT response originates from branches with endpoint energies of 4290.1 keV and 10420 keV. The pulse height spectrum from the PMT for ^{16}N and ^{32}P was obtained using a response function (10) and the data presented in Table 2. The situation in which all of the Cherenkov photons reach the photocathode of a PMT, i.e. light collection efficiency of 100%, is shown in Figure 7. In reality, even with good diffuse reflecting walls in a Cherenkov radiator, it is difficult to achieve high light collection efficiency. Similar calculations were obtained for light collection efficiency of 2 %, Figure 8. By comparing spectrum presented in Figures 7 and 8, it is possible to conclude, that the original good discrimination properties of the Cherenkov detector will be lost in case of low light collection efficiency. This also indicates, that low numbers of the distribution for a particular number to occur is no longer Gaussian but follows a Poisson distribution. The latter is asymmetrical at low numbers and tends to be Gaussian at high numbers. As a result, the pulse height spectrum from the PMT will be a distorted spectrum with long exponential tails.

By analyzing the tails of obtained pulse-height spectra of the ^{16}N and ^{32}P in the semilogarithmic scale, it was concluded that the slope of the most energetic half of pulse-height spectrum is an energy endpoint function of the β-emitter. In reality, for $x > (Q_0 + Q_{sh} + \mu Q_1)$ with a limited range of observation, the distribution can be represented this way:

$$S(x) \approx \frac{1}{\sqrt{2\pi\mu\left(\sigma_1^2 + Q_1^2\right)}} \cdot \exp\left(-\frac{x}{2\mu\left(\sigma_1^2 + Q_1^2\right)}\right). \tag{11}$$

In the similogarifmic scale, the slope of this function will be

$$\frac{d[\ln S(x)]}{dx} \approx \ln\left(\frac{1}{\sqrt{2\pi\mu\left(\sigma_1^2 + Q_1^2\right)}}\right) \cdot \left(-\frac{1}{2\mu\left(\sigma_1^2 + Q_1^2\right)}\right), \tag{12}$$

where the value μ, the number of photoelectrons, depends on the electron energy. The results of this analysis obtained for the case of light collection efficiency of 2% are shown in Figure 9. The correlation between the observed spectrum slope and the Cherenkov photon yield is shown in Figure 10. Slope of the pulse height spectrum is a function of the endpoint energy, $E_{\beta max}$, for each of the β-rays. Two of the observed slopes for the ^{16}N represent β-rays from the most intensive groups.

2.5. Interfering radionuclides

From the β-particles sufficient to cause Cherenkov radiation in water, the photon output increases rapidly with beta-energy to about 2 MeV (Figure 4), and further increases in energy result in smaller proportionate increases of light output. However, the number of β-particles of sufficient energy to cause high Cherenkov radiation in water increases markedly with the increase of maximum emission energy, due to the energy-spectrum characteristics of beta-emitters. Maximum energy of beta particles, from radionuclides induced by interaction of D-T neutrons with stable isotopes of hydrogen and oxygen found in pure water, is shown in Table 3. Only radioisotopes whose energy exceed the Cherenkov threshold in water, E_{th}=0,264MeV, are shown in the Table 3.

Table 3. Isotopes in the production of Cherenkov light in water irradiated by D-T neutrons.

Radioniclide	Half-life, [6] s	E^{β}_{Max}, [6] MeV	Reaction	Abundance, or. nuclide %	Cross section, [15] mb	Relative intensity, %
^{16}N	**7.13**	**10.4**	**$^{16}O(n,p)$**	**99.759**	**45**	**100**
^{15}C	2.449	9.77	$^{18}O(n,\alpha)$	0.204	7.6	0.10
^{17}N	4.173	8.68	$^{17}O(n,p)$	0.037	5.5	0.008
^{18}N	0.624	11.9	$^{18}O(n,p)$	0.204	2.3	0.12
^{19}O	29.91	4.63	$^{18}O(n,\gamma)$	0.204	0.1	0.0001

There are radionuclides (^{15}C, ^{17}N, ^{18}N) whose energies are very close to the energy of ^{16}N, however their appearances limit the abundance of the origin nuclide and the nuclear cross section. As a result, contribution of all nuclides to the Cherenkov signal from ^{16}N is less than 0.2%. Since the emitted Cherenkov light is roughly proportional to the beta particle energy, the ^{16}N can be instantly identified. Thus, the Cherenkov counter offers an advantage for counting ^{16}N in water. Explained briefly, it consists of selective detection of large light pulses originating from the passage of high-energy electrons in a volume of water.

3. Experimental studies and results

3.1. Equipment and experimental setup

The experiment was carried out using the 80^0 beamline at the FNS facility. The FNS accelerator was operated in a direct current mode. The main idea of the present experiment is to examine the measurement of the Cherenkov light by ^{16}N, using a water Cherenkov detector. For this purpose, radionuclide ^{16}N produced in the water near the D-T neutron source, was transported to the chamber of the Cherenkov detector using flowing water in the closed loop, with flow velocity of 2 m/s. Figure 11 shows the experimental setup. The water loop includes: the water reservoir, pump, flow meter, and the measuring chamber. In addition, two valves were installed in the water loop in order to change the direction of flowing water. In one position the water is flowing through the chamber, in the other case – directly to the water reservoir.

The chamber consists of an aluminum cylinder with dimensions of 5 cm in length, a 15 cm diameter, and a glass window, Figure 12 (a). To get uniform efficiency and good timing properties it is essential to have high reflectivity, and good diffusing properties of inside walls of the chamber. The inside walls were covered with 1mm thick Teflon sheets. The light collection in this chamber was far from the optimum, since the thickness of the reflecting Teflon layer must be more than 5 mm, with quartz as the material of the window. The photomultiplier, Hamamatsu R1250, was optically coupled to the window chamber, Figure 12 (b). For comparison purposes, a γ-ray scintillation ($Bi_4Ge_3O_{12}$) detector was located near the opposite side of the chamber. The chamber and the two detectors were shielded with 10 cm thick Pb blocks. The associated electronic package consists of a high voltage supply, signal amplifiers, and a multichannel analyzer, used for accumulating acquired counts within a selected window.

3.2. Test measurements of Cherenkov light by β-particles from ^{32}P in water

Prior to measurements of the Cherenkov light by β-rays from ^{16}N using a water Cherenkov detector, test and calibration measurements were completed for β-rays from ^{32}P. This specific nuclide was selected for a number of reasons. The main reason being the fact that the radionuclide is a pure β-emitter with relatively high energy endpoint, 1.7 MeV. Measurements were performed with the radionuclide ^{32}P, whose activity is known, in the same conditions as the measurements for the Cherenkov light by β-rays from ^{16}N. The evaluation of the Cherenkov counting efficiency for ^{32}P was the main goal in this measurement.

Radionuclide ^{32}P was produced via the $^{32}S(n,p)$ ^{32}P reaction utilizing natural abundance analytical grade dimetyl sylfone irradiated by D-T neutrons. Powder was pressed into pellets with a diameter of 13 mm and thickness of 2 mm. After D-T neutron irradiation of the sulfur-containing pellets, activity of the ^{32}P can be measured with a Cherenkov radiation detector, since this nuclide exhibits β-emission above 0.264 MeV of the threshold energy necessary for the excitation of Cherenkov radiation in water. In order to prepare the standard solution of ^{32}P, the irradiated pellets were dissolved in water. To eliminate the absorption effect of ^{32}P on the chamber walls, 1 g of inactive $NH_4PH_2O_2$ carrier was dissolved in water before the

dissolution of the pellets. The intensity and radionuclide purity of ^{32}P were confirmed by determining the half-life with the liquid scintillation method. Pellets, counted immediately after irradiation, show some short-lived impurities, the most significant of which is the 2.62-hour ^{31}S formed by the $^{34}S(n,\alpha)^{31}Si$ reaction. Allowing the pellets to decay for at least one day eliminates these activities. The ^{35}S ($T_{1/2}$ = 87 days) and ^{33}P ($T_{1/2}$ = 25.3 days) radionuclides, that can be formed in the pellet, have no counts due to the Cherenkov threshold in water. With these precautions, the measured β-activity is found to decay with the half-life appropriate to ^{32}P.

For the purpose of measuring the Cherenkov light by β-rays from ^{32}P using a water Cherenkov detector, the chamber was filled with ^{32}P water solution. The water Cherenkov detector was investigated with respect to its response to ^{32}P, at several phototube voltages and amplifier gains. The typical pulse height spectrum is shown in Figure 13. For the high energy part of the spectrum, the curve happens to have a near-exponential shape, and is nearly linear on the semilogarithmic plot of the type shown in Figure 13.

The discrimination level was set to a level corresponding to pulses arising from electrons with energy of about 1 MeV. The value of the set discrimination level is discussed in paragraph 3.5. In this case, the Cherenkov counting efficiency for ^{32}P was estimated to be around 5.2%.

3.3. Measurements of Cherenkov light by β-particles from ^{16}N in water

The ^{16}N radionuclide was generated by D-T neutron irradiation of water flowing next to the source in the position of a neutron flux of about $1 \cdot 10^8$ n/cm^2/s. The transit time to the Cherenkov radiation detector was ~ 6 sec. For the production of ^{16}N and measurements of Cherenkov light by β-particles from ^{16}N in water, equipment arranged according to the experimental setup presented in the paragraph 3.1 was used. In these measurements the appropriate discrimination level was set up for elimination of most of the signals arising from Compton electrons, produced from γ-ray interactions in the neutron activated water. The pulse height spectrum is shown in Figure 14.

3.4. Identification of the registered Cherenkov signal

The registered Cherenkov signal from ^{16}N was identified using the time decay and the pulse height distribution spectrum. In the experimental run, the water flow in the chamber was stopped and the time decay was estimated. It fully corresponds to the decay time of ^{16}N. The obtained experimental result is shown in Figure 15.

Pulse-height spectra of ^{16}N and ^{32}P (for comparison) are shown in Fig.16. The slope of the most energetic half of the pulse-height spectrum is a function of the $E_{\beta max}$ for each beta emitter. ^{32}P has only one β-decay branch ($E_{\beta max}$=1710 keV), thus the highly energetic part of the experimental spectrum corresponds to one slope. The result of the deconvolution of ^{16}N spectrum is also shown in Fig.16. Two obtained slopes correspond to major β-decay branches of the ^{16}N, with endpoint energies of $E_{\beta max}$= 4290 keV and $E_{\beta max}$= 10420 keV (Table 2).

3.5. Evaluation of the counting efficiency

The method evaluating the Cherenkov counting efficiency of ^{16}N is based on the modified idea originally proposed by Grau Carles and Grau Malonda[16]. This idea separates the counting efficiency into two terms: the yield and the intrinsic Cherenkov counting efficiency. Thus, the counting efficiency can be expressed as follows:

(13)

$$\varepsilon_{Ch} = \eta \cdot \varepsilon_{Int} .$$

The yield, η, i.e. the ratio between particles emitted over the set energy threshold, E_{th}, and the total number of emitted particles, can be obtained directly from β-ray distribution by:

(14)

$$\eta = \frac{\int_{E_{th}}^{E_{max}} N(E)dE}{\int_{0}^{E_{max}} N(E)dE} .$$

The intrinsic Cherenkov counting efficiency, ε_{Int}, is defined as the ratio between counted particles and emitted particles over the set energy threshold:

(15)

$$\varepsilon_{Int} = \frac{k\int_{E_{th}}^{E_{max}} N(E)f(E)dE}{\int_{E_{th}}^{E_{max}} N(E)dE},$$

where: E_{max} and E_{th} - the maximum and set threshold β-ray energies, respectively;
$N(E)$ - the β-ray distribution;
k – light collection efficiency;
$f(E)$ - detection probability.

It is assumed, that the response of the spectrometer to monoenergetic radiation is unique for electrons with kinetic energies over the Cherenkov threshold. If the measurement conditions and the equipment will not vary, the detection probability function is assumed to be identical for every electron emitter. The detection of high-energy electrons by Cherenkov light depends only on the established measurement conditions. According to the solution[16], the function f(E) is unity for β-rays with sufficient energy for total detection; that is, the detection probability of nearly 1 for electrons .of E > 1MeV in water. This energy value was used in all measurements performed in this study, as the lower energy threshold. For this case, the intrinsic Cherenkov counting efficiency was evaluated with the ^{32}P radionuclide.

The dependence of the yield, η, on the energy threshold was calculated for ^{32}P and ^{16}N. The results are presented in Figure 17. For the set threshold energy of 1 Mev, the calculation of the yields gives the value of 20.6 % for ^{32}P and 85.9 % for ^{16}N.

Taking into consideration the experimental value of Cherenkov counting efficiency obtained for ^{32}P, 5.2%, from equation (13), the intrinsic Cherenkov counting efficiency for the used detector was evaluated to be 25.2%. The application of the obtained value to other nuclides requires maintenance of the measurement conditions applied to the measurement of the ^{32}P radionuclide. For the same instrumental conditions, it is possible to use this value for evaluation of the Cherenkov counting efficiency for ^{16}N. Thus, the Cherenkov counting efficiency for ^{16}N is 22.2%. As was expected, measurements of the ^{32}P and ^{16}N have shown that the utilized camera is not optimized for measurements of the Cherenkov light and requires modification.

4. Comparison of the neutron monitoring techniques for D-T fusion reactor

The main neutron monitoring techniques for the D-T fusion reactor are listed in Table 4. Three basic techniques exist:

1. Solid sample activation and rabbit system[17];
2. Fission rate measurements by fission chamber[18];
3. Activation of flowing water and subsequent measurements of induced ^{16}N activity[5].

The new technique, proposed and discussed in the present study is basically a modification of the third technique, that allows to significantly improve key parameters of the technique. By comparing the data shown in Table 4, it is concluded that all the presented techniques are able to control the fusion power in the requested range. Neutron activation technique utilizing solid metal samples is used for most accurate measurements of the neutron yield in many fusion devices, however without temporal resolution.

Only two of the existing techniques can control the reactor power: the fission chamber and the proposed technique. It is expected that the time resolution in the proposed technique will be less than 50 ms. Existence of the remote detector allows to effectively service it. On the other hand, it is impossible to do such kind of maintenance with the fission chamber. The new technique is sensitive only to D-T neutrons, while the fission chamber is also sensitive to γ-rays. It is possible to build such a detector on the basis of the new technique that will be insensitive to variations in the plasma profile and position of the plasma. By comparing the techniques listed in Table 4, it is possible to conclude that the proposed technique potentially possesses all the advantages of the other techniques. In addition, the detector can be easily scaled to large volumes in order to increase the detection efficiency.

5. Future work

In order to complete the feasibility study of the Cherenkov detector as a D-T fusion power monitor, the second experimental phase is scheduled for execution. The main idea of the second experimental phase consists of:

1) studying the temporal resolution of the proposed technique;
2) finding the optimal solution of transmitting the Cherenkov signal in conditions of heavy neutron radiation.

The second experimental phase is proposed to create appropriate experimental conditions, which would allow research of the technique's parameters. Temporal resolution, sensitivity of the technique and the linearity of response are to be studied as a result of this phase. For purposes of the study, a special Cherenkov detector is to be created, consisting of a water radiator, an optical fiber, and a remotely located light detector. It is proposed that the water radiator is to be placed next to the D-T neutron source, and the Cherenkov light generated in the water radiator from the β- rays of the ^{16}N, will then be transferred by an optical fiber to the remotely located light detector. All the obtained results will allow to complete research of the proposed technique's main parameters.

6. Conclusions

For the purpose of monitoring D-T neutrons in the system, using neutron activation of flowing water, a new approach was proposed. It enables to solve problems associated with the response delay and temporal resolution, which are the most important drawbacks of the previous approach. The basic idea of the new approach is to utilize the Cherenkov light, which is produced by energetic β-particles from ^{16}N in water near the first wall of the fusion reactor, and then transmit it by the optical fiber to the remote light detector. In support of this idea, the first experimental phase was completed. During the experiment, the radionuclide ^{16}N generated in the water flowing past the D-T neutron source, was transported to the remotely located Cherenkov detector. The response of the detector to the Cherenkov light from the ^{16}N was studied comprehensively. It was concluded, that the water Cherenkov detector is very effective in measuring the ^{16}N activity, due to: high counting efficiency, a maximum theoretical value of 98%; absence of the scintillation detector; and simplicity of the method. The present study elaborates upon the feasibility and effectiveness of utilizing the Cherenkov radiation detector in the D-T neutron monitoring system.

Acknowledgments

The authors gratefully acknowledge the operation staffs, C. Kutsukake, S. Tanaka, Y. Abe, M. Seki and Y. Oginuma, for their good operation of the D-T neutron source at the FNS facility.

References

1) Perez-Griffo M.L., Block R.C., and Lahey R.T., "Measurement of Flow in Large Pipes by the Pulsed neutron Activation Method," Nucl. Sci. Eng., 82, 19 (1982).
2) Nakagawa T., Kawasaki H., and Shibata K.,: "Curves and Tables of Neutron Cross Sections in JENDL –3.3. Part I (Z=1-50)" JAERI-Data/Code, 2002-020, Japan Atomic Energy research Institute, (2002).
3) Ikeda Y., Uno Y., Maekawa F., Smith D.L., Gomes I.C., Ward R.C., Filatenkov A.A., "An Investigation of the Activation of water by D-T fusion neutrons and some Implications for Fusion reactor Technology", Fusion Engineering and Design, 37, 107 (1997).
4) Nishitani T., Ebisawa K., Walker C., Kasai S., "Desigh of Neutron monitor Using Flowing water Activation for ITER", JAERI-Tech, 2002-033, Japan Atomic Energy research Institute, (2002).
5) Nishitani T., Ebisawa K., and Kasai S., and Walker C., "Neutron activation system using water flow for ITER", Rev. Sci. Instrum., Vol. 74, No.3, pp. 1735-1738 (2003).
6) Firestone R. B., Shirley V.S. (Ed.) Table of Isotopes, 8th Edition, John Wiley & Sons, Inc., New York, 1996.
7) Cherenkov P.A., "Visible glow of pure liquids under the influence of γ-rays" Dokl. Akad. Nauk. SSSR, 2, p.451 (1934).
8) Cherenkov P.A., "Visible radiation produced by electrons moving in a medium with velocities exceeding that of light", Phys.Rev. 52, 378 (1937).
9) Frank I.M., Tamm I.G., "Coherent visible radiation of fast electrons passing throught matter" Dokl. Akad. Nauk. SSSR. 14, 109 (1937).
10) Mukoyama T., "Range of electrons and positrons", Nucl. Instr. and Methods, 134, 125 (1976).
11) Ross H.H., "Measurement of β-emitting nuclides using Cerenkov radiation", Analytical Chemistry, Vol.41, No. 10, pp.1260-1265 (1969).
12) Wu C.S., Moszkowski S.A., "Beta decay", John Wiley & Sons, Inc., 1966.
13) Chu S.F., Ekström L.P., and Firestone R.B., WWW Table of Radioactive Isotopes, 1999, http://ie.lbl.gov/toi/.

14) Bellamy E.H., "Absolute calibration and monitoring of a spectrometrical channel using a photomultiplier", Nucl. Instr. and Methods, A 339, pp. 468-476 (1994).

15) Victoria McLane, Charles L. Dunford, and Philip F.Rose, Neutron Cross Section, Vol. 2, NNDC, BNL, Academic Press, 1988.

16) Grau Carles A., Grau Malonda A., "Radionuclide Standardization by Cherenkov Counting", Appl. Radiat. Isot. Vol.46, No. 6, pp. 799-803 (1995).

17) Barnes C. W., Loughlin M. J., Nishitani T., "Neutron activation for ITER", Rev. Sci. Instrum., Vol. 68, No.1, pp. 577-580 (1997).

18) Yamauchi M., Nishitani T., Ochiai K., Morimoto Y., Hori J., Ebisawa K., Kasai S., and Walker C., "Development of in-vessel neutron monitor using micro-fission chambers for ITER", Rev. Sci. Instrum., Vol. 74, No.3, pp. 1730-1734 (2003).

Table 4. D-T neutron monitor techniques for the fusion reactor

Status		Presently used			Proposed
Parameter/Function \ Principle		Solid Sample Activation & Rabbit System	Fission Chamber	Flowing water activation & γ-ray detector	Flowing water activation & Cherenkov detector
Measurement range of neutron flux ($10^{+13} - 10^{+20}$) n/s		Yes	Yes	Yes	Yes
Reactor control		No	Yes	No	Yes[1]
Temporal resolution		No	1ms	~ 50 ms[2]	Better than 50 ms [1]
Accuracy of absolute monitoring		< 5 %	< 10 %	< 10 %	< 10 %
Long-term stability		High	Low	High	High
Remote detector		Yes	No	Yes	Yes
Sensitivity:	Neutrons	Yes	Yes	D-T neutrons only	D-T neutrons only
	Plasma profile/position	Yes	Yes	No	No [1]
	Gamma-ray field	No	Yes	No	No [1]
	Electromagnetic field	No	Yes	No	No

[1] To be studied in detail in the second experimental phase
[2] Depends on the water flow velocity and location of the remote detector.

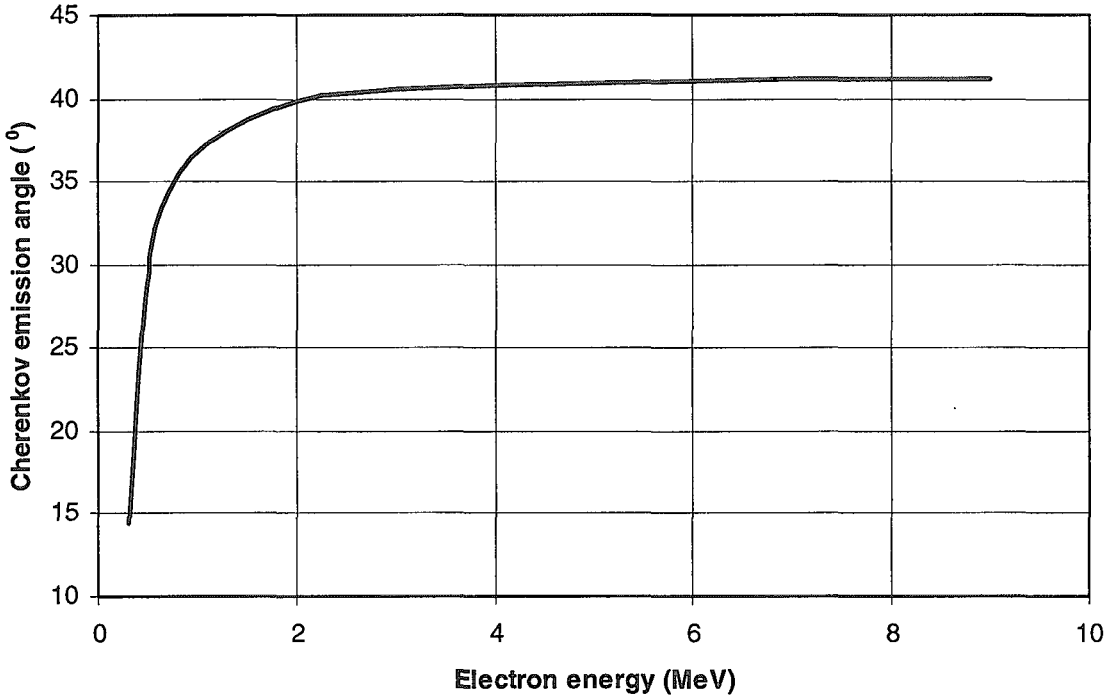

Figure 1. Cherenkov emission angle as a function of electron energy

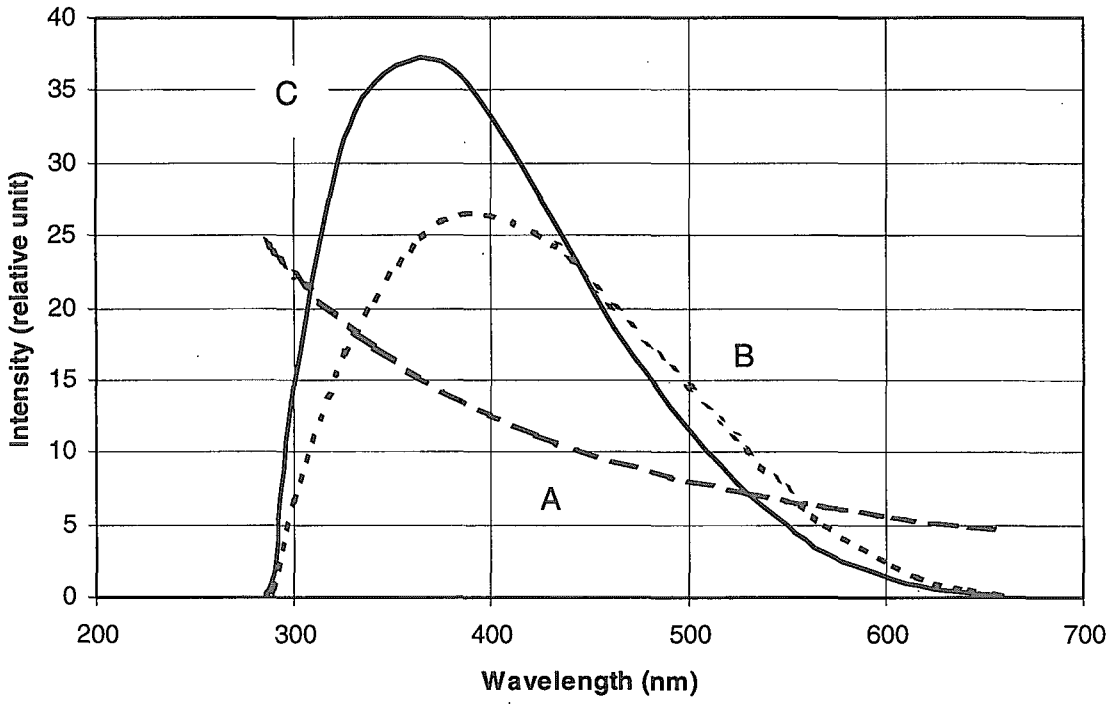

Figure 2. A – Emitted Cherenkov spectrum, displaying the $1/\lambda^2$ dependence; B – Spectral effective quantum efficiency of the photomultiplier tube (Hamamatsu, R1250) used in the Cherenkov counter; C – Predicted differential spectral response of the photomultiplier tube to Cherenkov radiation.

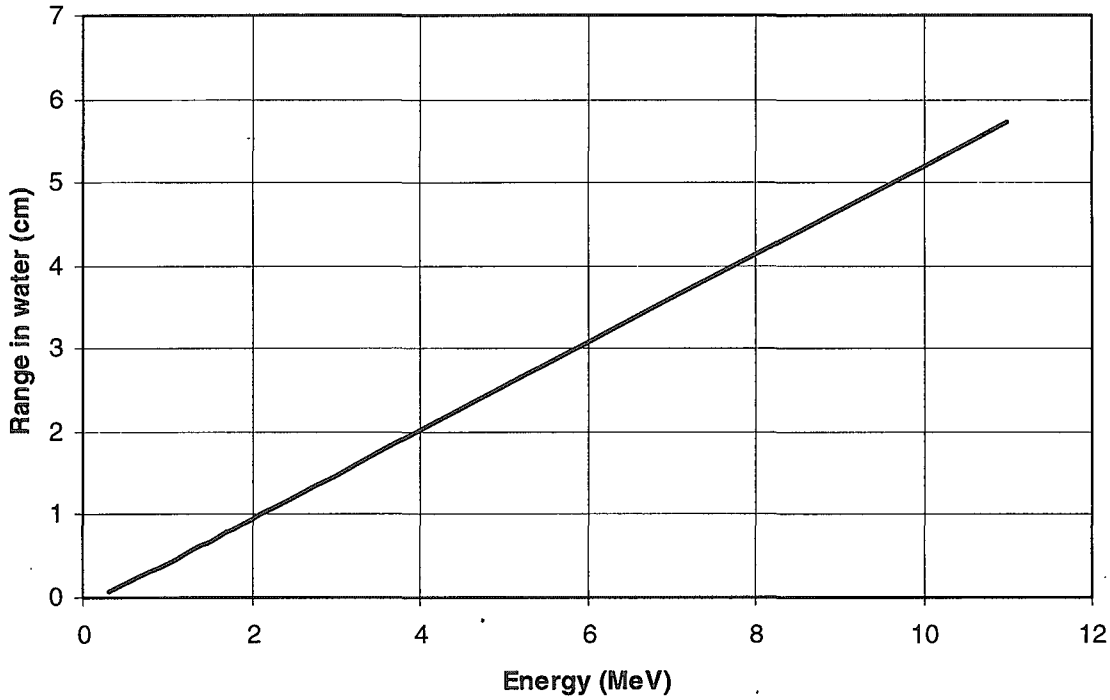

Figure 3. The range of electrons in water.

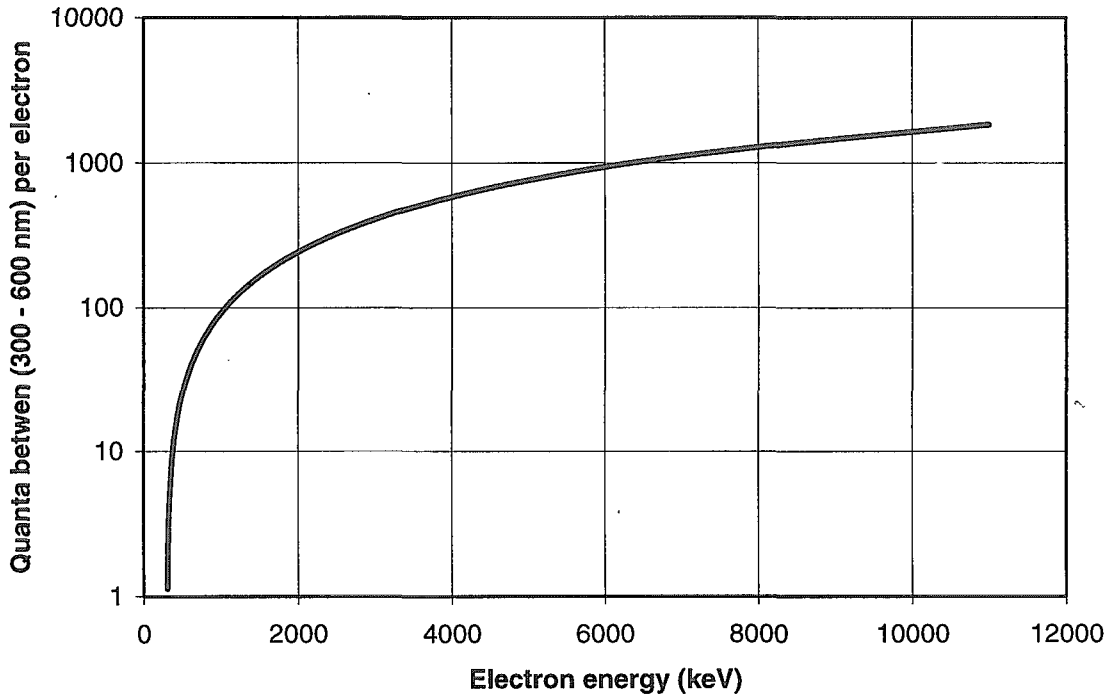

Figure 4. The number of Cherenkov photons emitted per electron as a function of electron energy, calculated for the spectral region of 300-600 nm.

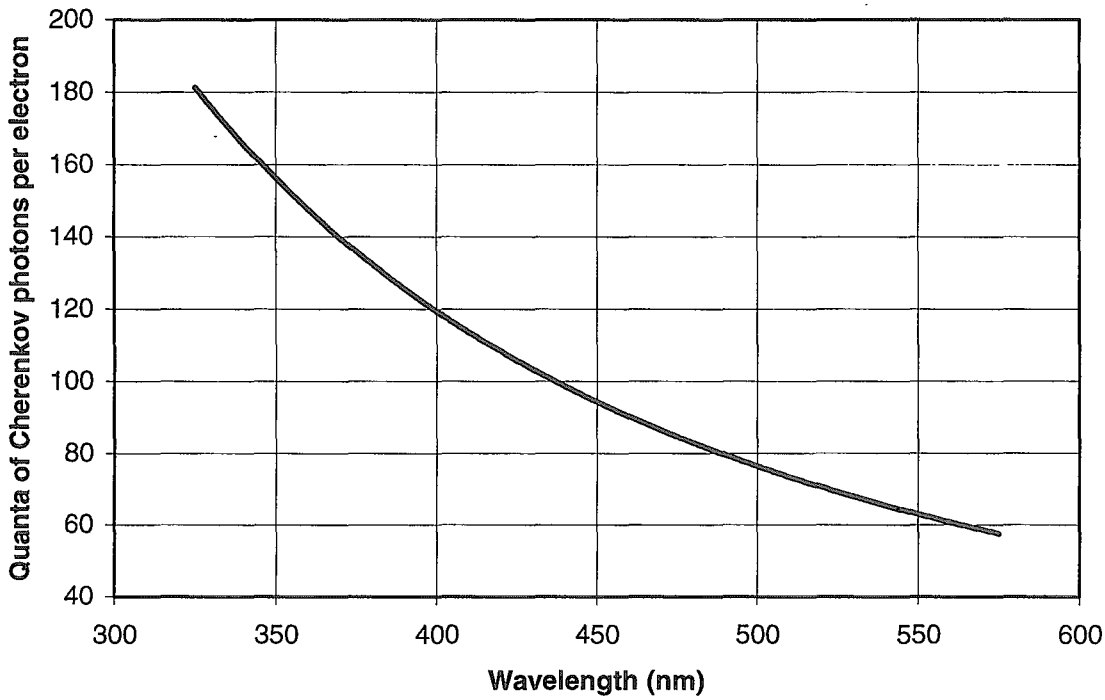

Figure 5. Cherenkov photon spectra in water for an electron with a maximum energy of 4MeV

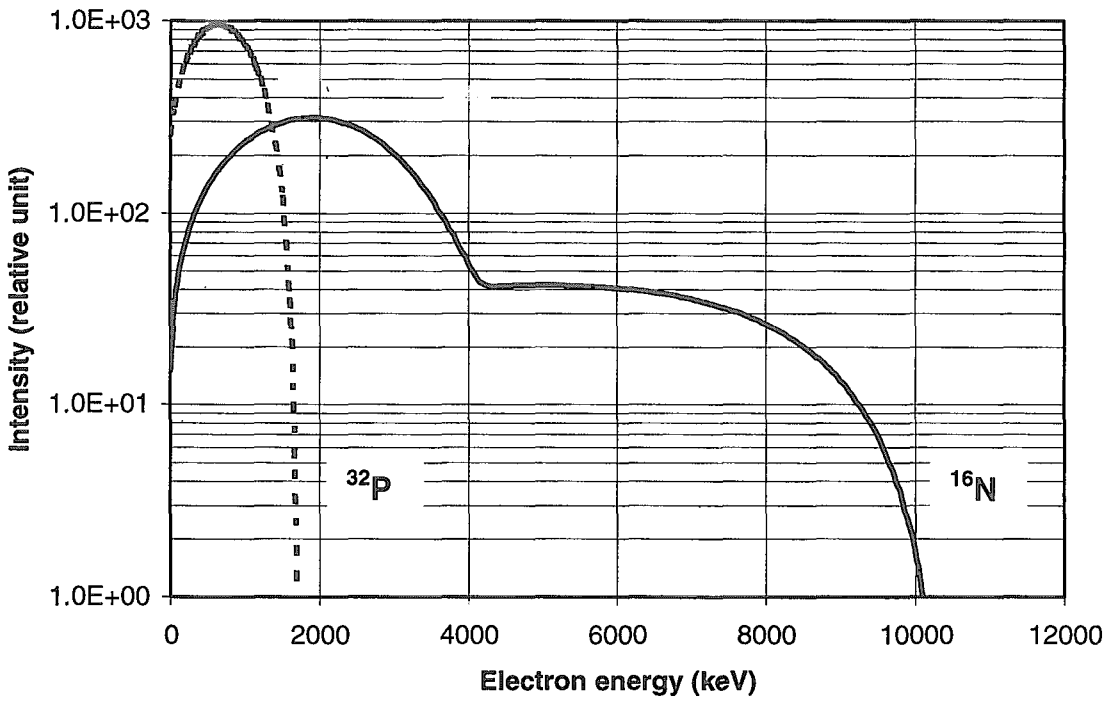

Figure 6. Beta spectrum of ^{16}N and ^{32}P radionuclides .

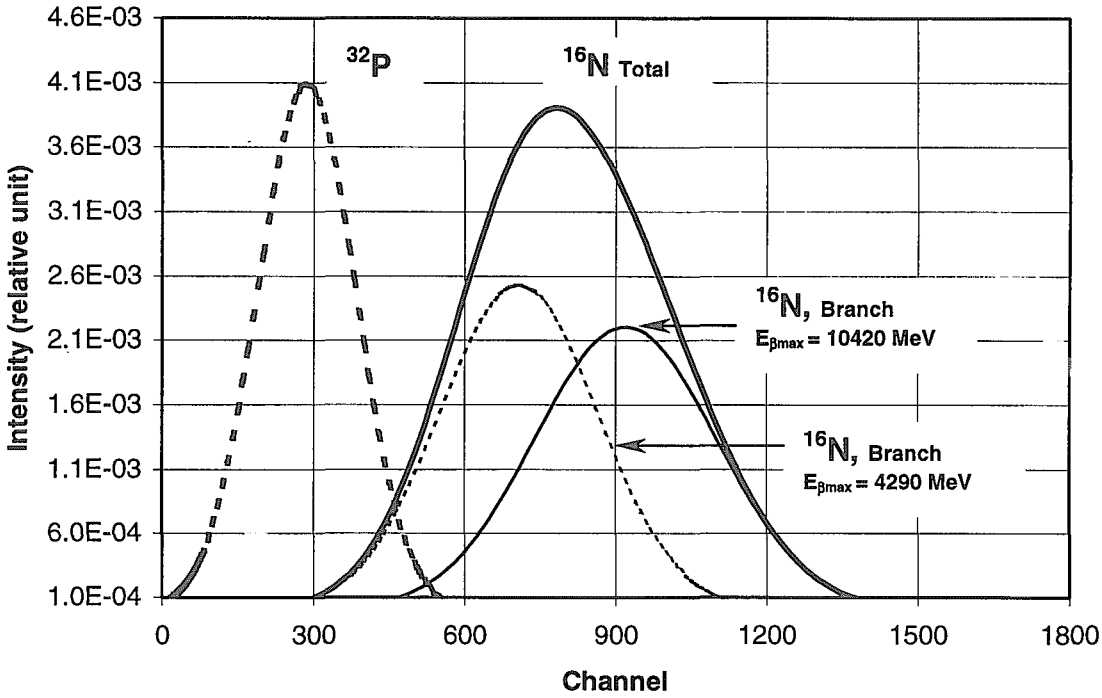

Figure 7. The simulated PMT response to Cherenkov photons generated in water from β-rays of ^{32}P and ^{16}N radionuclides. Light collection efficiency – 100%.

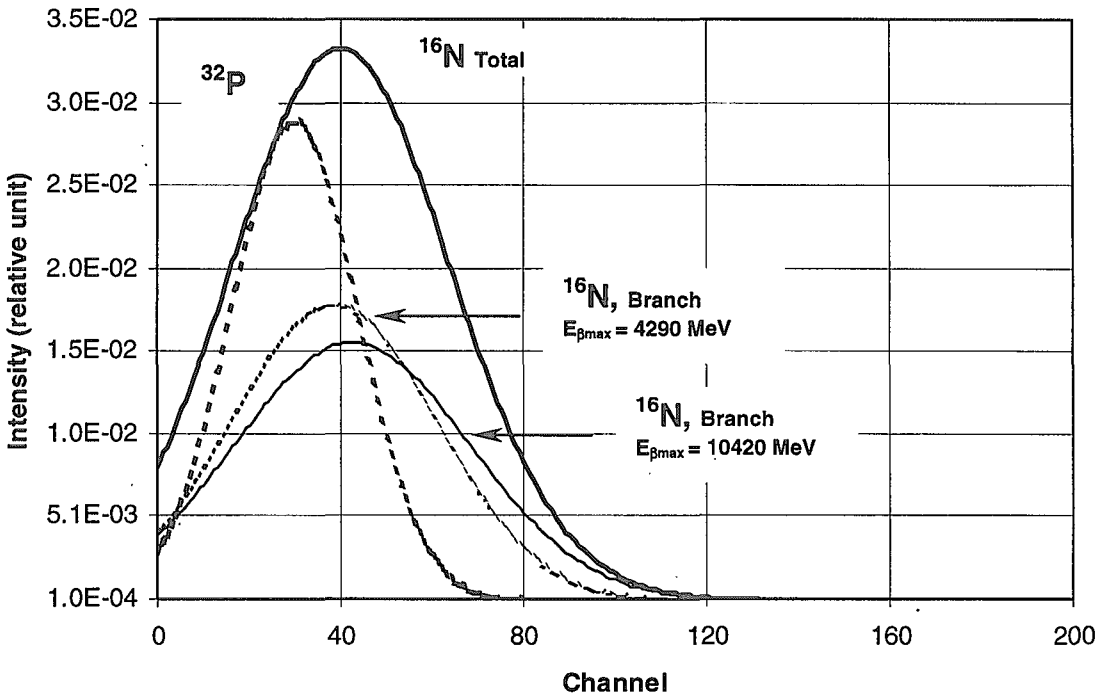

Figure 8. The simulated PMT response to Cherenkov photons generated in water from β-rays of ^{32}P and ^{16}N radionuclides. Light collection efficiency – 2%.

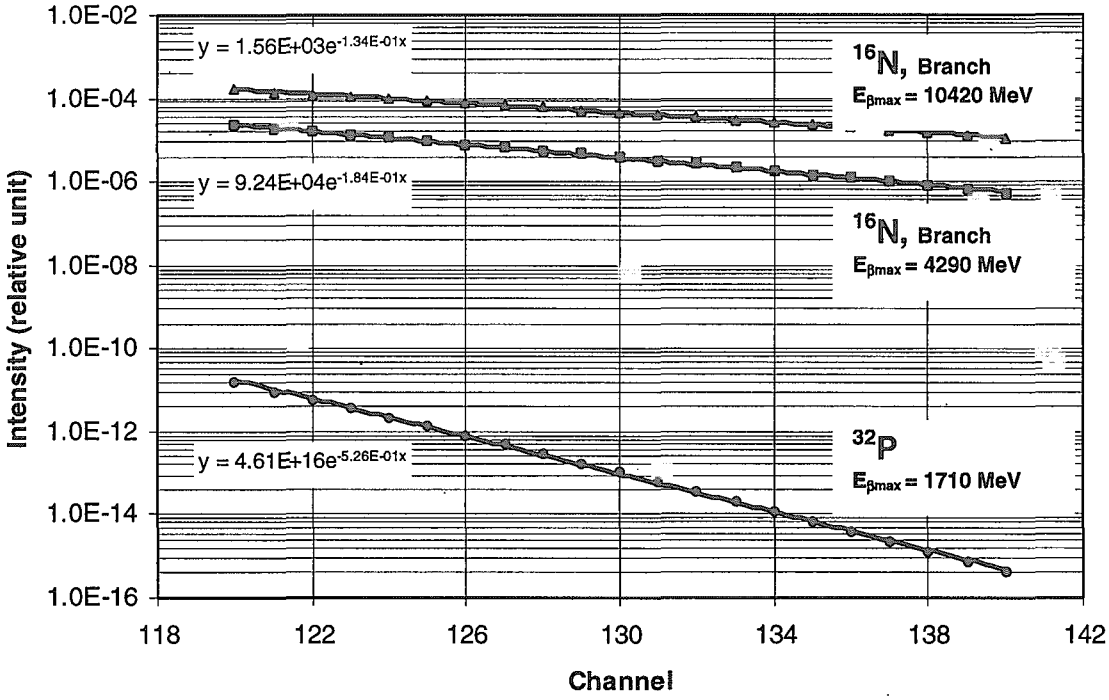

Figure 9. Tails of the pulse height spectra of PMT responses to Cherenkov photons generated in water from β-rays of ^{32}P and ^{16}N radionuclides.

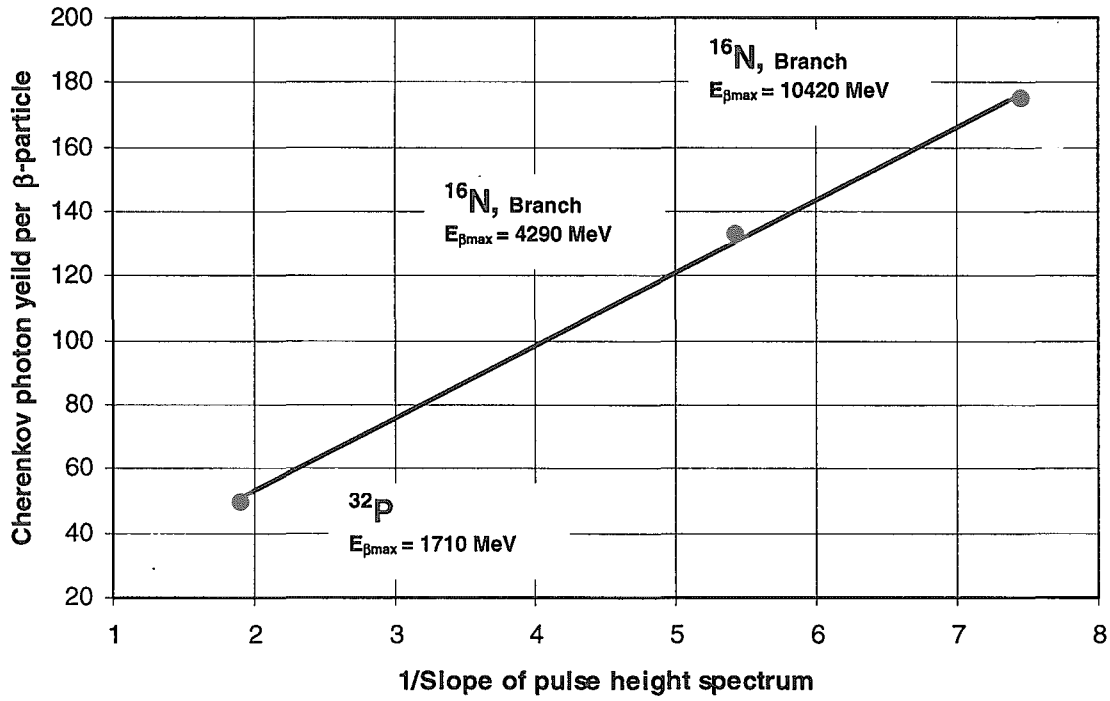

Figure 10. Cherenkov photon yield as a function of the pulse height spectrum slope.

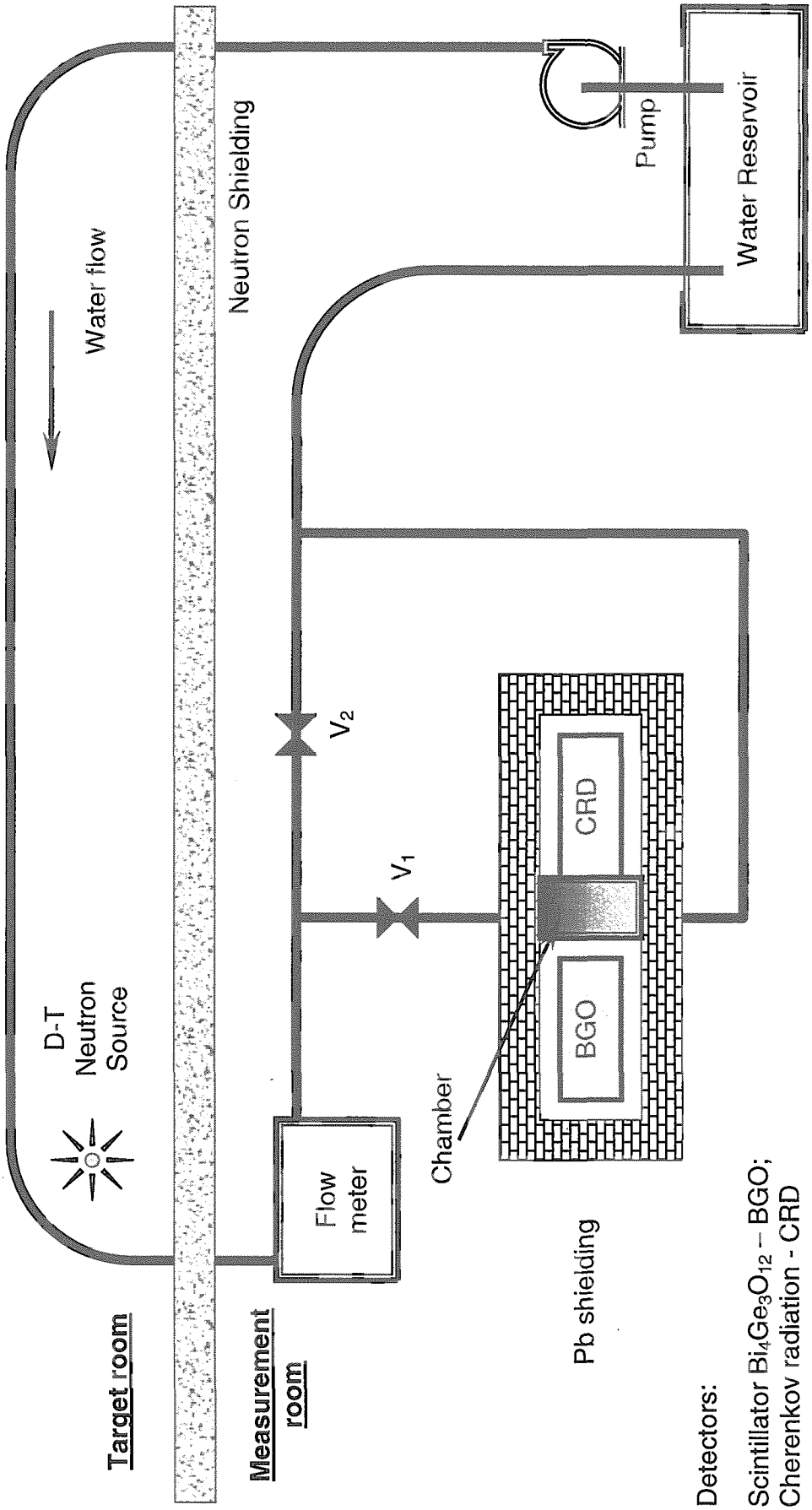

Figure 11. Overview of apparatus used in the ^{16}N production and measurement experiment

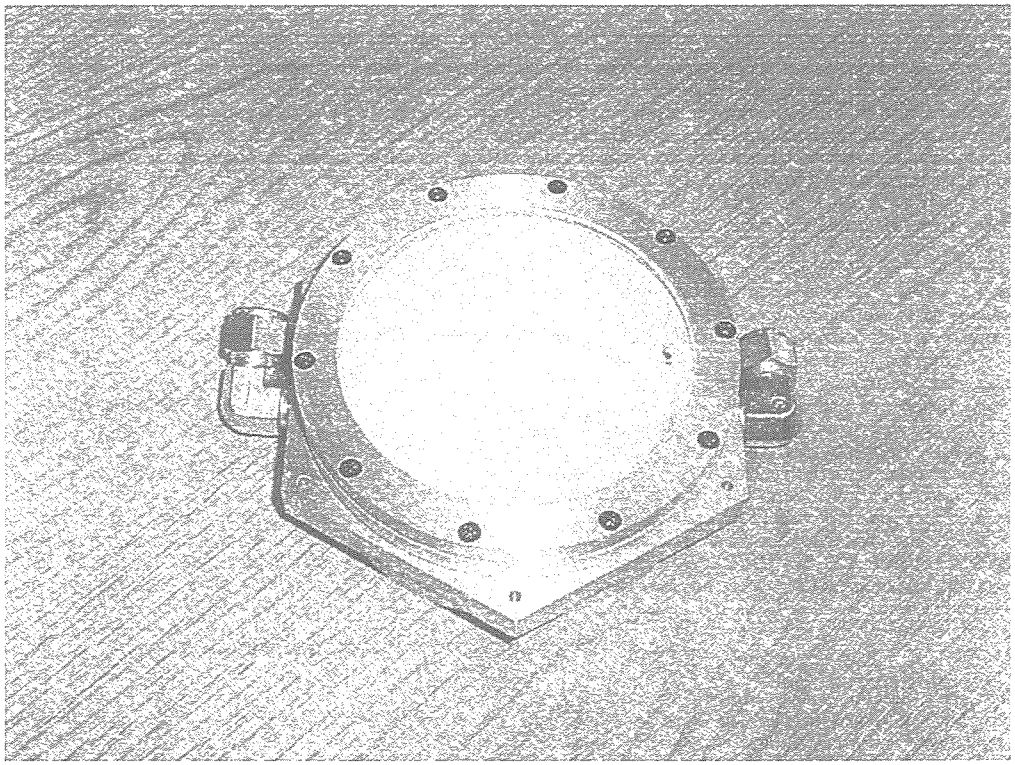

a) Optical chamber

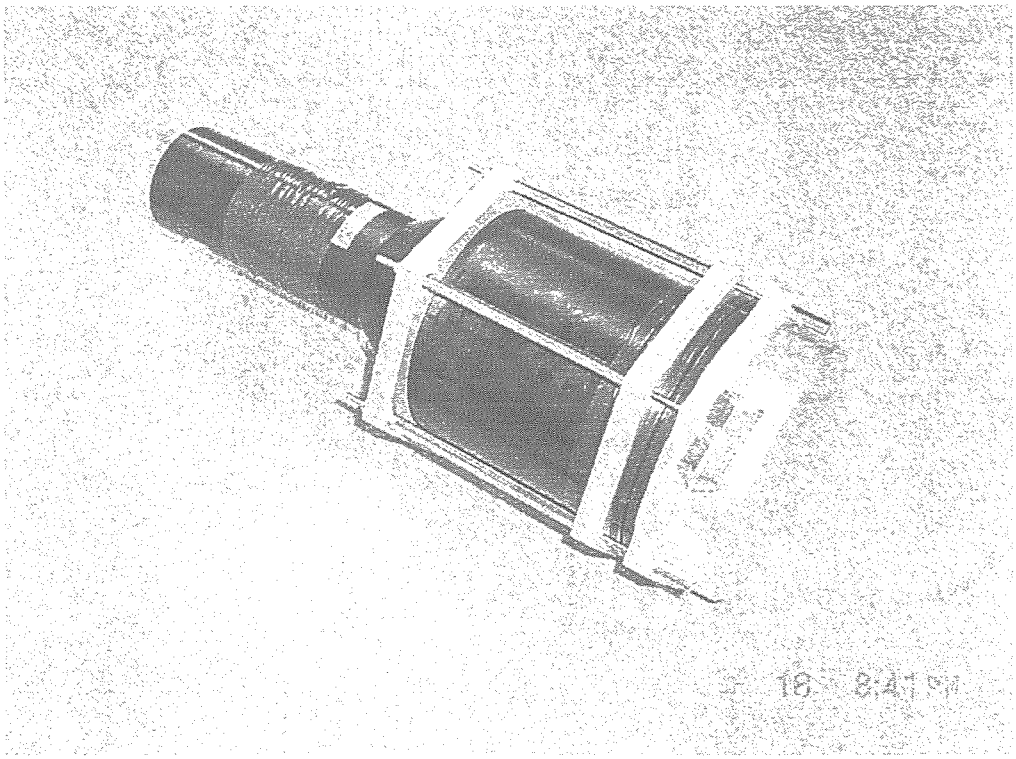

b) Chamber coupled with PMT

Figure 12. The detector for measuring Cherenkov light by β-rays from ^{16}N

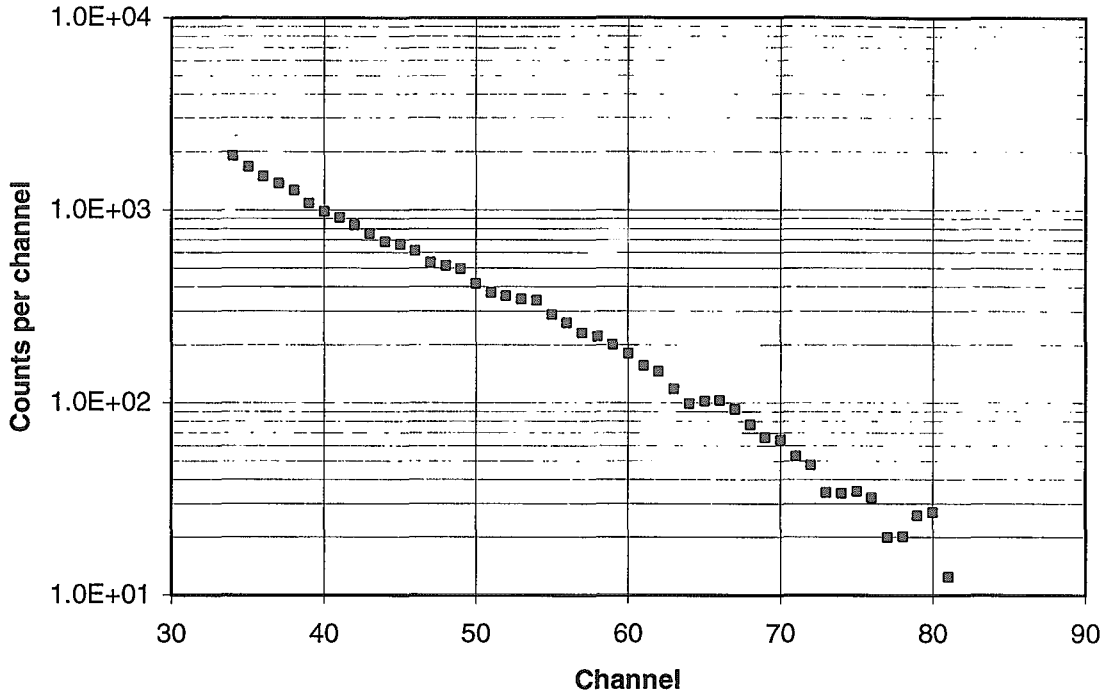

Figure 13. Pulse height spectrum of ^{32}P measured using the water Cherenkov detector

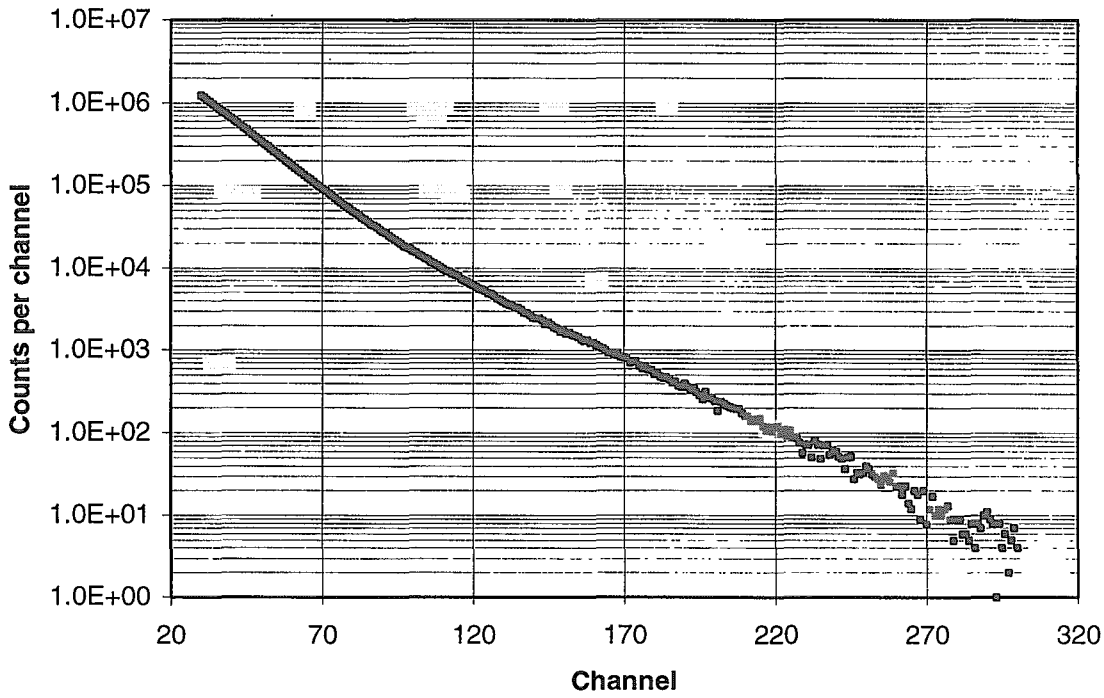

Figure 14. Pulse height spectrum of ^{16}N measured using the water Cherenkov detector

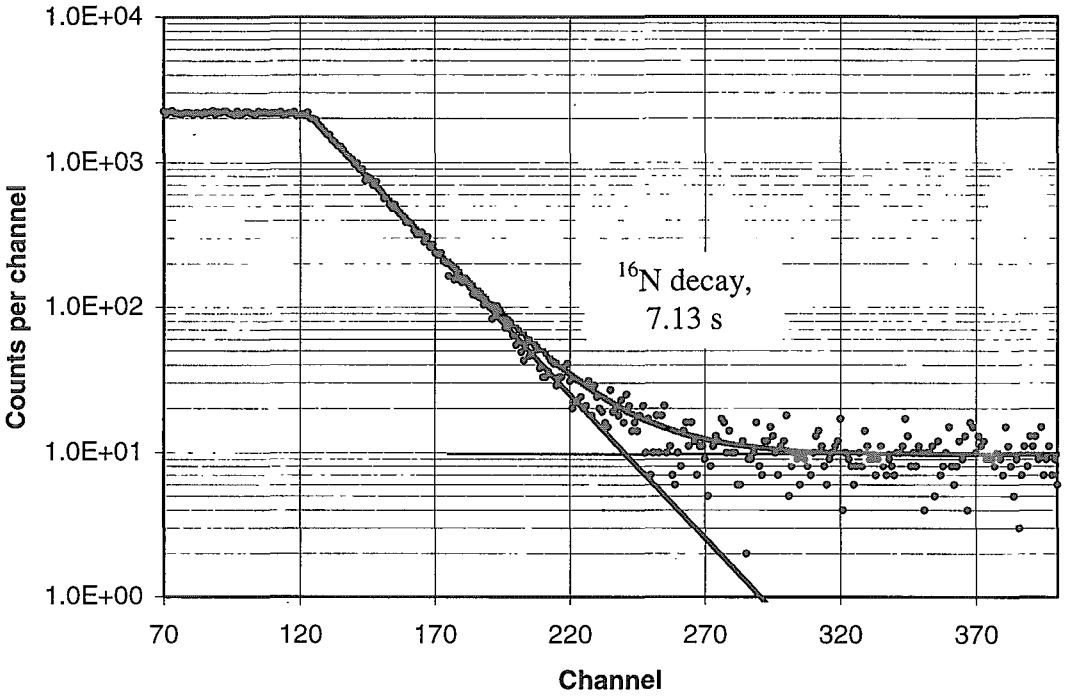

Figure 15. Intensity of the Cherenkov signal from ^{16}N as a function of cooling time

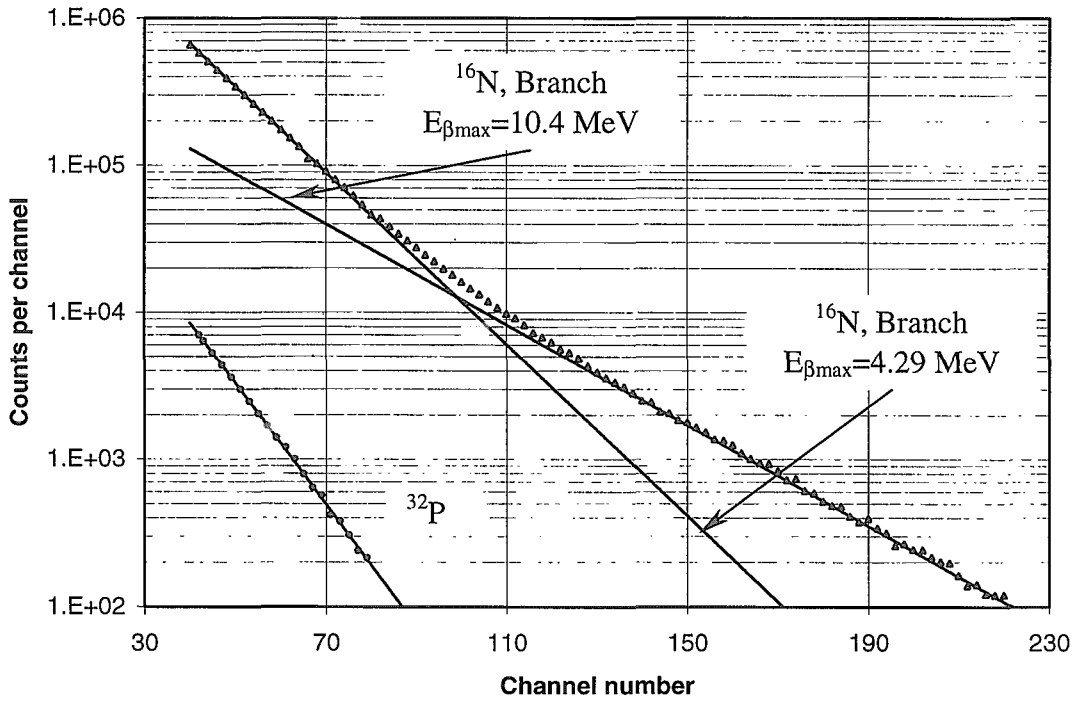

Figure 16. The deconvoluted pulse height spectrum of ^{16}N measured by the water Cherenkov detector. Spectrum of ^{32}P is shown for comparison.

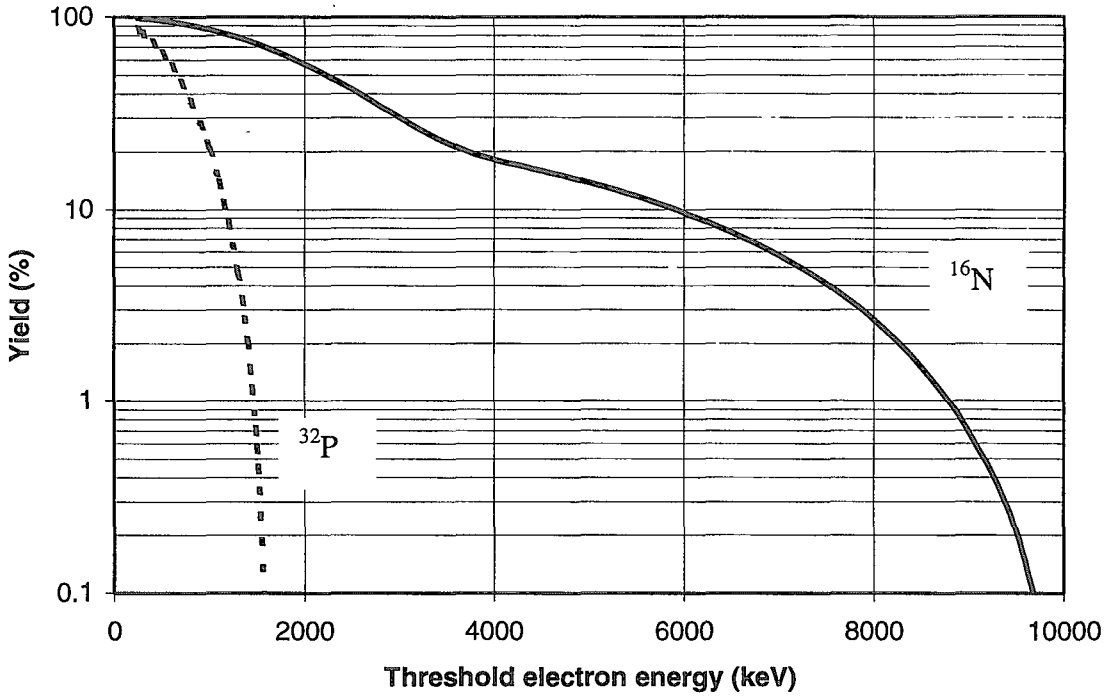

Figure 17. Dependence of the Cherenkov yield on the threshold electron energy

This is a blank page.

国際単位系 (SI) と換算表

表1　SI基本単位および補助単位

量	名称	記号
長さ	メートル	m
質量	キログラム	kg
時間	秒	s
電流	アンペア	A
熱力学温度	ケルビン	K
物質量	モル	mol
光度	カンデラ	cd
平面角	ラジアン	rad
立体角	ステラジアン	sr

表2　SIと併用される単位

名称	記号
分，時，日	min，h，d
度，分，秒	°，′，″
リットル	l，L
トン	t
電子ボルト	eV
原子質量単位	u

1 eV=1.60218×10^{-19} J

1 u=1.66054×10^{-27} kg

表3　固有の名称をもつSI組立単位

量	名称	記号	他のSI単位による表現
周波数	ヘルツ	Hz	s^{-1}
力	ニュートン	N	m·kg/s^2
圧力，応力	パスカル	Pa	N/m^2
エネルギー，仕事，熱量	ジュール	J	N·m
工率，放射束	ワット	W	J/s
電気量，電荷	クーロン	C	A·s
電位，電圧，起電力	ボルト	V	W/A
静電容量	ファラド	F	C/V
電気抵抗	オーム	Ω	V/A
コンダクタンス	ジーメンス	S	A/V
磁束	ウェーバ	Wb	V·s
磁束密度	テスラ	T	Wb/m^2
インダクタンス	ヘンリー	H	Wb/A
セルシウス温度	セルシウス度	℃	
光束	ルーメン	lm	cd·sr
照度	ルクス	lx	lm/m^2
放射能	ベクレル	Bq	s^{-1}
吸収線量	グレイ	Gy	J/kg
線量当量	シーベルト	Sv	J/kg

表4　SIと共に暫定的に維持される単位

名称	記号
オングストローム	Å
バーン	b
バール	bar
ガル	Gal
キュリー	Ci
レントゲン	R
ラド	rad
レム	rem

1 Å= 0.1 nm=10^{-10} m

1 b=100 fm^2=10^{-28} m^2

1 bar=0.1 MPa=10^5 Pa

1 Gal=1 cm/s^2=10^{-2} m/s^2

1 Ci=3.7×10^{10} Bq

1 R=2.58×10^{-4} C/kg

1 rad=1 cGy=10^{-2} Gy

1 rem=1 cSv=10^{-2} Sv

表5　SI接頭語

倍数	接頭語	記号
10^{18}	エクサ	E
10^{15}	ペタ	P
10^{12}	テラ	T
10^{9}	ギガ	G
10^{6}	メガ	M
10^{3}	キロ	k
10^{2}	ヘクト	h
10^{1}	デカ	da
10^{-1}	デシ	d
10^{-2}	センチ	c
10^{-3}	ミリ	m
10^{-6}	マイクロ	μ
10^{-9}	ナノ	n
10^{-12}	ピコ	p
10^{-15}	フェムト	f
10^{-18}	アト	a

（注）

1. 表1－5は「国際単位系」第5版，国際度量衡局 1985年刊行による。ただし，1 eVおよび1 uの値はCODATAの1986年推奨値によった。
2. 表4には海里，ノット，アール，ヘクタールも含まれているが日常の単位なのでここでは省略した。
3. barは，JISでは流体の圧力を表わす場合に限り表2のカテゴリーに分類されている。
4. EC閣僚理事会指令ではbar，barnおよび「血圧の単位」mmHgを表2のカテゴリーに入れている。

換　算　表

力	N(=10^5dyn)	kgf	lbf
	1	0.101972	0.224809
	9.80665	1	2.20462
	4.44822	0.453592	1

粘度　1 Pa·s(N·s/m^2)=10 P(ポアズ)(g/(cm·s))

動粘度　1 m^2/s=10^4St(ストークス)(cm^2/s)

圧力	MPa(=10 bar)	kgf/cm^2	atm	mmHg(Torr)	lbf/in^2(psi)
	1	10.1972	9.86923	7.50062×10^3	145.038
	0.0980665	1	0.967841	735.559	14.2233
	0.101325	1.03323	1	760	14.6959
	1.33322×10^{-4}	1.35951×10^{-3}	1.31579×10^{-3}	1	1.93368×10^{-2}
	6.89476×10^{-3}	7.03070×10^{-2}	6.80460×10^{-2}	51.7149	1

エネルギー・仕事・熱量	J(=10^7erg)	kgf·m	kW·h	cal(計量法)	Btu	ft·lbf	eV
	1	0.101972	2.77778×10^{-7}	0.238889	9.47813×10^{-4}	0.737562	6.24150×10^{18}
	9.80665	1	2.72407×10^{-6}	2.34270	9.29487×10^{-3}	7.23301	6.12082×10^{19}
	3.6×10^6	3.67098×10^5	1	8.59999×10^5	3412.13	2.65522×10^6	2.24694×10^{25}
	4.18605	0.426858	1.16279×10^{-6}	1	3.96759×10^{-3}	3.08747	2.61272×10^{19}
	1055.06	107.586	2.93072×10^{-4}	252.042	1	778.172	6.58515×10^{21}
	1.35582	0.138255	3.76616×10^{-7}	0.323890	1.28506×10^{-3}	1	8.46233×10^{18}
	1.60218×10^{-19}	1.63377×10^{-20}	4.45050×10^{-26}	3.82743×10^{-20}	1.51857×10^{-22}	1.18171×10^{-19}	1

1 cal = 4.18605 J（計量法）

= 4.184 J　（熱化学）

= 4.1855 J　（15 °C）

= 4.1868 J（国際蒸気表）

仕事率　1 PS（仏馬力）

= 75 kgf·m/s

= 735.499 W

放射能	Bq	Ci
	1	2.70270×10^{-11}
	3.7×10^{10}	1

吸収線量	Gy	rad
	1	100
	0.01	1

照射線量	C/kg	R
	1	3876
	2.58×10^{-4}	1

線量当量	Sv	rem
	1	100
	0.01	1

（86年12月26日現在）

Feasibility Study of the Water Cherenkov Detector as a D-T Fusion Power Monitor in the System using Neutron Activation of Flowing Water - First Experimental Phase -

古紙配合率100%
白色度70%の再生紙を使用しています